Magneto-optic properties and ferromagnetism of (In,Mn)As/(In,Al)As/(Ga,Al)Sb heterostructures

P. Fumagalli
2. Physikalisches Institut, Rheinisch-Westfälische Technische Hochschule Aachen, D-52056 Aachen, Germany

H. Munekata
Imaging Science and Engineering Laboratory, Tokyo Institute of Technology, 4259 Nagatsuda, Midori-ku, Yokohama 226, Japan
(Received 4 October 1995)

Reflectivity and polar Kerr-rotation measurements of (In,Mn)As/(Ga,Al)Sb-based diluted-magnetic-semiconductor heterostructures over a photon-energy range of 0.7–3 eV in magnetic fields up to 3 T are presented. The spectra were taken at a temperature of 5.5 K well below the ferromagnetic ordering temperature of ~35 K. The distinct energy gaps of individual layers in a heterostructure lead to very structured reflectivity and polar Kerr spectra. Based on a model calculation, a correlation between local minima in the reflectivity and peak position in the Kerr spectra is established. Magneto-optic hysteresis loops reveal a large squareness reaching 100% in some samples. In addition, Kerr spectra in the remanent state are almost identical to spectra in a saturating magnetic field indicating that paramagnetic contributions are unimportant and the entire Kerr spectra is dominated by interband transitions involving ferromagnetically ordered spins. From a detailed analysis it is concluded that these interband transitions originate exclusively from transitions involving Mn $3d$ local moments within the (In, Mn)As layer. From the dependence of the magneto-optic properties on (In, Mn)As thickness, a correlation between lattice mismatch and perpendicular magnetic anisotropy is confirmed. The influence on the ferromagnetic exchange of an (In,Al)As interlayer between the (In,Mn)As/AlSb interface is demonstrated to reduce perpendicular magnetic anisotropy but not to destroy ferromagnetic ordering in the (In,Mn)As layer. [S0163-1829(96)01522-6]

INTRODUCTION

Diluted magnetic semiconductors (DMS) are suitable for studying magnetic and electronic properties as well as cooperative effects caused by spin-exchange interaction between conduction carriers and local magnetic moments. The successful demonstration of epitaxial growth of (In,Mn)As thin films[1–5] has provided the opportunity to investigate a new class of technologically important III-V DMS. Taking advantage of III-V semiconductor properties and fabrication technology, it is possible to control the type and number of carriers over a wide range and, most importantly, to design heterostructures to change average distance between carriers and local magnetic moments.

A good example demonstrating the interplay between conduction carriers and local magnetic moments in the III-V DMS is the striking perpendicular ferromagnetic order in p-type (In,Mn)As/(Ga,Al)Sb heterostructures which is believed to be caused by carrier (hole)-induced ferromagnetism.[6–8] The (In,Mn)As/AlSb system shows a ferromagnetic transition at $T_C \cong 35$ K with strong perpendicular magnetic anisotropy.[6,7] From the Hall resistance of $In_{0.88}Mn_{0.12}As(d_{MS})$/AlSb(0.1–0.3 μm)/GaSb(0.3–1.0 μm) heterostructures it is concluded that ferromagnetism dominates only in a narrow thickness regime of $d_{MS}=5$–20 nm.[8] Similar results are found in (In,Mn)As/$Ga_{1-y}Al_ySb$ heterostructures in the entire range $0 \leqslant y \leqslant 1$.[8] However, in (In,Mn)As/$AlSb_{1-z}As_z$ structures perpendicular ferromagnetism is significantly weaker and vanishes completely at $z \cong 0.15$. At this As concentration a nearly lattice-matched condition between the constituent layers is established. As a result, the occurrence of perpendicular magnetic anisotropy can be attributed to strain-induced crystal anisotropy by a lattice mismatch of 0.6–1.3 % between (In,Mn)As and (Ga,Al)Sb layers.[8]

In this work we examine the magneto-optic properties of (In,Mn)As/(In,Al)As/(Ga,Al)Sb III-V DMS heterostructures and discuss the dependence of ferromagnetism on structure parameters such as the thickness of the (In,Mn)As layer and the influence of an (In,Al)As spacer layer on the long-range magnetic order. Concerning the spacer-layer dependence, we intend to clarify the conjecture of a potential ferromagnetic exchange across the (In,Mn)As/AlSb interface as suggested by previous experiments.[6] Magneto-optic spectroscopy is shown in this work to be a magnetic-layer-specific method with which we can focus on the exchange within the ferromagnetic (In,Mn)As top layer. This is in contrast to magneto-transport experiments where carriers (holes) existing not only in the (In,Mn)As but also in the nonmagnetic AlSb layers are contributing to the transport effects. Therefore, the influence of those carriers which are involved in the magnetic exchange might be small. First results have been published before[9] showing for a heterostructure a strong magneto-optic effect with a maximum Kerr rotation of 0.18° at 1.65 eV.

EXPERIMENTAL

The heterostructures investigated were all grown by molecular-beam epitaxy (MBE). A typical layering sequence is sketched in Fig. 1. All nonmagnetic III-V layers were grown at substrate temperatures $T_s=480$–580 °C. The semi-insulating GaAs(100) substrate is first covered with 300 nm GaAs for smoothing the substrate surface. In a second step, a

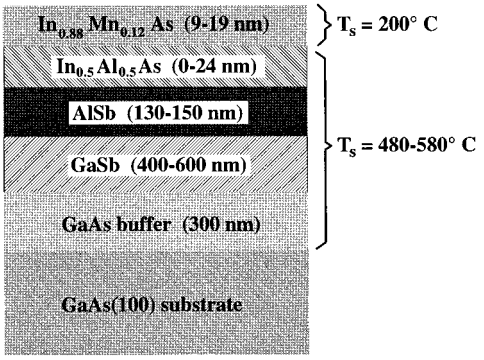

FIG. 1. Sketch of the layering sequence in (In,Mn)As heterostructures grown by MBE. The GaAs(100) substrate is semi-insulating. A 300 nm thick GaAs layer is for smoothing the substrate surface while a 400–600 nm thick GaSb layer is used to accommodate the large lattice mismatch between GaAs and AlSb which has a relatively good lattice match to (In,Mn)As.

GaSb buffer layer of 400 nm is added in order to reduce the large lattice mismatch between the AlSb and the GaAs layers. An AlSb layer is grown next with a thickness of 100–200 nm. Finally, the DMS $In_{1-x}Mn_xAs$ layer is deposited at T_s=200 °C with $x \cong 0.12$ and with a thickness of 9–19 nm. To study the influence of a potential barrier between the magnetic (In,Mn)As and the AlSb layer on the ferromagnetic exchange, an $In_{0.5}Al_{0.5}As$ spacer layer of thickness up to 24 nm was grown in between. The low-T_s growth yields a homogeneous (In,Mn)As alloy in the zinc-blende structure without a macroscopic ferromagnetic MnAs second phase as confirmed by TEM measurements.[10] A schematic phase diagram is plotted in Fig. 2.

Polar Kerr-rotation measurements were performed on a fully automated high-resolution Kerr spectrometer using a standard lock-in technique,[11] in which the light-polarization direction is modulated at a low frequency of ~80 Hz using a Faraday modulator. The light was incident onto the (In,Mn)As side of the samples at an angle of less than 5° from the normal. The photon-energy range extended from 0.7 to 3 eV. As light sources a 100 W tungsten halogen lamp for the infrared part and a 150 W xenon high-pressure lamp for the visible and ultraviolet part of the spectrum were used. An Oxford optical cryostat with a split-coil superconducting magnet provided magnetic fields up to 7 T at temperatures down to 4.2 K. In order to account for the Faraday rotation of cryostat windows and other optical components within the stray field of the magnet, a reference measurement with an aluminum mirror (Kerr rotation negligible) was done first. The result was subtracted from the sample measurement yielding a corrected Kerr rotation of the sample. To cancel the influence of any birefringence of nonmagnetic origin (e.g., stress-induced), all measurements were taken in both positive and negative magnetic fields and then averaged. Polar Kerr hysteresis loops were taken in a similar way on the same setup.

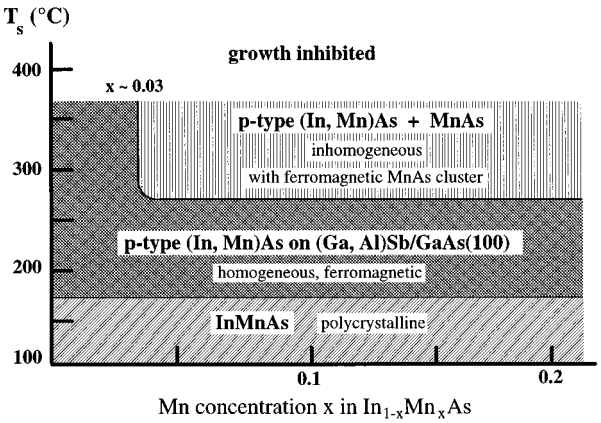

FIG. 2. Schematic diagram showing the physical properties of (In,Mn)As grown on (Ga,Al)Sb/GaAs(100) in relation to the two growth parameters, substrate temperature, and Mn composition. Lines are meant to be a rough guide.

Reflectivity measurements were done with unpolarized light relative to an aluminum reference mirror and thereafter corrected with tabulated data for aluminum.[12] Therefore, the magnitude of the reflectivity spectra shown in this work might include an error of a few percent but the relative size and position of the features in the spectra are not affected by this procedure.

OPTICAL RESULTS (REFLECTIVITY)

It has to be emphasized at this point that it is not the purpose of this study to make an unambiguous assignment of the features in the reflectivity spectrum as one would need a thorough analysis of the optical properties of the heterostructures for that. The idea is rather to understand qualitatively how DMS-layer thickness and spacer-layer thickness influence the reflectivity. This is important for the comprehension of the magneto-optic properties of the III-V DMS heterostructures as the polar Kerr rotation strongly depends on the optical functions n (index of refraction) and k (index of absorption) as will be discussed below.

The individual layers of the heterostructures are mostly semiconducting. Their thicknesses are except for the GaAs substrate less than the wavelength of the incident light. Therefore, the reflectivity spectra are expected to be dominated by structures relating to the direct energy gaps of individual layers and by interference effects. Table I collects for the heterostructures investigated in this work the direct energy gap, E_g^{dir}, at low temperatures,[13] and the thickness of the individual layers. Within the energy range covered in this work, only AlSb and (In,Al)As are transparent up to ~2 eV. Therefore, we can divide the energy range into two sections.

Below 2 eV, structures can originate only from electronic transitions in the (In,Mn)As and the GaSb layers. Interference effects are only to be expected from the AlSb and the GaSb layers because the (In,Mn)As and the (In,Al)As layers are too thin. The critical thickness, d_{int}, for a constructive optical-interference effect in reflection is roughly given by

$$2nd_{\mathrm{int}} = (2j+1)\,\frac{\lambda}{2}, \tag{1}$$

where n is the index of refraction of a transparent material, λ is the wavelength of the light, and j is an integer. This formula is valid for a free-standing layer facing air. A phase shift of 180° at the front surface and none at the back surface is taken into account. In the heterostructures, the situation is

TABLE I. Direct energy gap and thickness of the individual layers of the heterostructures.

Direct gap E_g^{dir} at 4.2 K (Ref. 13)	$In_{0.88}Mn_{0.12}As$ ~0.42 eV	$In_{0.5}Al_{0.5}As$ ~1.77 eV	AlSb 2.32 eV	GaSb 0.81 eV	GaAs 1.52 eV
*R*1350	9 nm	0 nm	136 nm	400 nm	300 nm
*R*1351	9 nm	0 nm	0 nm	600 nm	300 nm
*R*1356	9 nm	3.5 nm	140 nm	600 nm	300 nm
*R*1357	9 nm	7 nm	140 nm	600 nm	300 nm
*R*1385	19 nm	0 nm	145 nm	600 nm	300 nm
*R*1388	18.5 nm	24 nm	145 nm	600 nm	300 nm

much more complicated because the layers are either not transparent or they are facing an absorbing layer instead of air. Yet, Eq. (1) is appropriate for a rough estimate. Taking $d_{int}=20$ nm and n between 2–4, we get an interference wavelength $\lambda=160-320$ nm which is more than 3 eV in photon energy. Therefore, such thin layers as the (In,Mn)As or the (In,Al)As layers do not show an interference effect within the energy range covered in this work. The GaAs layer and substrate will not contribute to the reflectivity spectra as the penetration depth of the light is not deep enough. Above 2 eV, no interference effects will be present any more and electronic transitions may arise from all layers including AlSb and (In, Al)As.

The reflectivity spectrum at a temperature of 5.5 K of the simplest heterostructure, (In,Mn)As/GaSb with a DMS-layer thickness of 9 nm, is shown in Fig. 3. Several features can be distinguished, labeled *A* through *D*. By referring to an analysis[14] of the optical properties of InAs and GaSb, an assignment of some of the structures is attempted. The most prominent peak *A* is assigned to an $\mathbf{E_1}$ transition (notation according to Ref. 13) in GaSb at 2.15 eV which appears as a sharp kink at 2 eV in the absorption spectra.[14] We may further assign structure *B*, which is lowest in energy, to the direct band gap $E_g^{dir}=0.8$ eV in GaSb. At slightly higher photon energies, three peaks are found, C,C',C'', with an equal energy spacing of 0.25 eV whose amplitudes decrease monotonically with increasing photon energy. They could be explained in terms of interference within the GaSb layer. Using Eq. (1), neglecting absorption ($k\cong 0$), and assuming $n=4$ for GaSb,[13] an energy separation of 0.26 eV of the interference maxima is calculated for a 600 nm thick GaSb layer, in good agreement with the energy separation of the structures C-C''. On the other hand, the absorption coefficient, K_{GaSb}, is larger than 2×10^4 cm^{-1} above 1 eV yielding a penetration depth of the light of less than 500 nm. Therefore, the argument that the C-C'' peaks are due to an interference effect is a rather tentative conclusion at present. Features *D* and *D'* are found in all heterostructures independent of the underlying layers. It is tempting to assign them to the (In,Mn)As layer. However, it should be noted that such features have not been observed in 2.5 μm thick (In,Mn)As films.[9]

In Fig. 4 we plot the reflectivity spectra at a temperature of 5.5 K for two (In,Mn)As/AlSb heterostructures with DMS-layer thicknesses of 9 and 19 nm. The structures are labeled *A* through *E*. Most features are present in both heterostructures. Peak *A* and *B* are not shifted whereas *D* and *D'* are shifted towards lower energy in the sample with a thicker DMS layer. Features *C* and *C'* are not present in the thicker DMS sample which has a single structure *E* at slightly higher energy. Peak *A* is assigned to E_g^{dir} in AlSb as it is close to $E_g^{dir}=2.32$ eV and does not shift in the two samples. Features *B*, *C*, and *C'* cannot be assigned unambiguously. Interference maxima due to the AlSb layer are expected to be separated by 1.35 eV ($n=3.3$, $k\cong 0$). The only feature at that energy is peak *C'*. But the sample with thicker DMS layer does not exhibit a peak at that energy although the AlSb-layer thickness is almost the same.

The influence of an (In,Al)As-spacer layer on the reflectivity spectra is depicted in Fig. 5. Structures *B*, *D*, and *D'* appear at about the same energy as in the samples without spacer layer (Fig. 4) whereas the main feature *A* is shifted to lower energy but does not show a dependence on spacer-

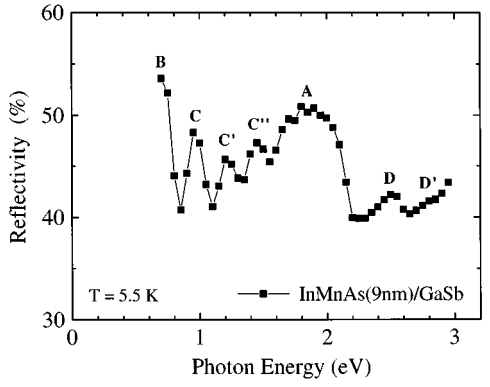

FIG. 3. Reflectivity spectrum of an $In_{0.88}Mn_{0.12}As$(9 nm)/GaSb(600 nm) heterostructure.

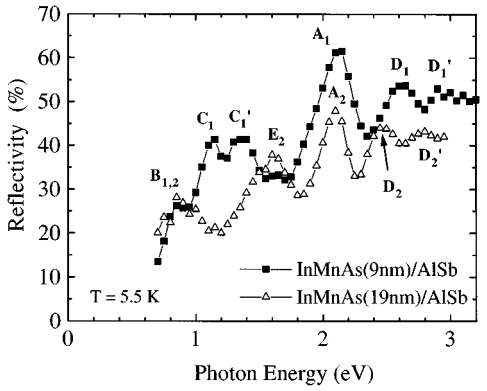

FIG. 4. Reflectivity spectra of two $In_{0.88}Mn_{0.12}As$/AlSb heterostructures with $In_{0.88}Mn_{0.12}As$-layer thickness $d_{MS}=9$ nm (■) and 19 nm (△).

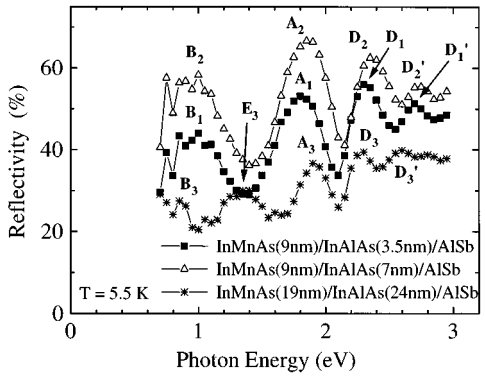

FIG. 5. Reflectivity spectra of $In_{0.88}Mn_{0.12}As/In_{0.5}Al_{0.5}As/AlSb$ heterostructures with different $In_{0.5}Al_{0.5}As$-layer thickness d_{sp}=3.5 nm (■), 7 nm (△), and 24 nm (∗).

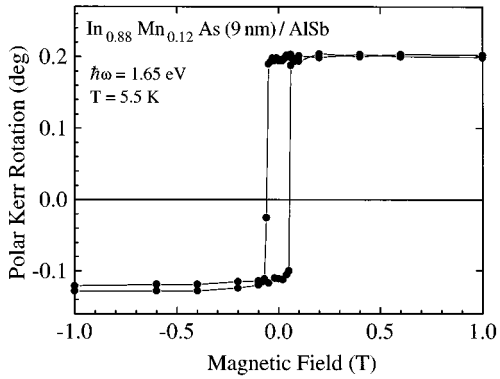

FIG. 7. Polar Kerr hysteresis loop at 5.5 K of an $In_{0.88}Mn_{0.12}As$(9 nm)/AlSb(136 nm) heterostructure at a photon energy $\hbar\omega$=1.65 eV.

layer thickness. This is in accordance with a lower E_g^{dir} =1.77 eV in (In,Al)As as compared to AlSb. Consequently, peak A is associated with E_g^{dir} in (In,Al)As. Structures C and C' from Fig. 4 are not present. Peak E only appears in the sample with thicker DMS layer as seen in both Figs. 4 and 5. This suggests that peak E might be due to a Mn transition as they have a larger oscillator strength in thicker DMS layers.

MAGNETO-OPTIC RESULTS

Polar Kerr-rotation spectra of an $In_{0.88}Mn_{0.12}As$(9 nm)/AlSb(136 nm) heterostructure are shown in Fig. 6 at a temperature of 5.5 K which is well below the Curie temperature $T_C \cong 35$ K. The spectrum in a high magnetic field of 3 T [Fig. 6(a)] where magnetic saturation is achieved is almost identical to the spectrum in the remanent state [Fig. 6(b)]. This

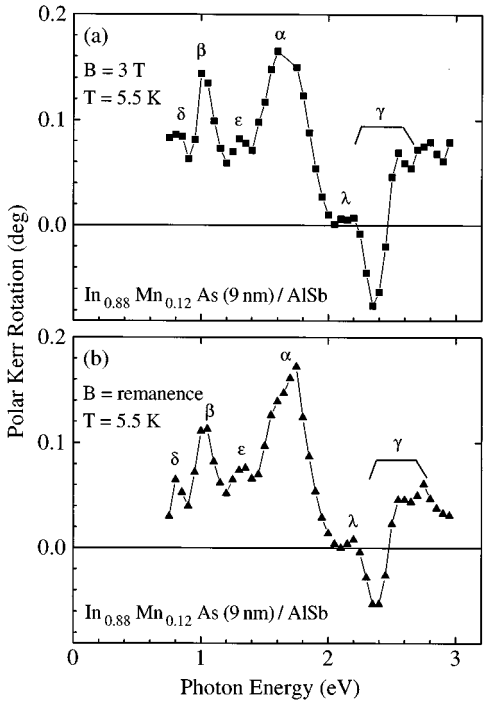

FIG. 6. Polar Kerr-rotation spectra at 5.5 K of an $In_{0.88}Mn_{0.12}As$(9 nm)/AlSb(136 nm) heterostructure in (a) a field of 3 T and (b) in the remanence state as a function of photon energy.

indicates that paramagnetic contributions are negligible and the whole spectrum is related to spin-polarized electronic transitions which can solely be due to Mn 3d local moments. The Kerr spectra show three distinct features. At 1.65 eV (peak α), the Kerr rotation θ_K reaches a maximum value of 0.18°. A small structure β appears at 1 eV. Finally, an S-shaped structure, labeled γ, is observed at 2.5 eV. Besides these dominant features, some very small peaks (δ,ε,λ) arise at 0.8, 1.3, and 2.15 eV, respectively, reflecting the rich structure of the reflectivity spectrum (Fig. 4).

Ferromagnetic order is nicely demonstrated in polar Kerr hysteresis loops as plotted in Fig. 7. The loop was taken at a photon energy $\hbar\omega$=1.65 eV corresponding to the maximum θ_K. The heterostructure exhibits strong perpendicular magnetic anisotropy also found in Hall measurements[8] yielding a squareness $\theta_K^{rem}/\theta_K^{sat}=1$. The high squareness is also reflected in the similarity of the remanent spectra with the one at 3 T. A small coercive field H_c=0.055 T is deduced from Fig. 7. The displacement of the hysteresis loop by 0.05° is due to intrinsic birefringence of the sample which originates from stress in the layers due to, e.g., lattice mismatch. Such birefringence leads to an extra field-independent rotation of the light-polarization direction.

In Fig. 8, we show the polar Kerr-rotation spectra for two different heterostructures to point out the sensitive dependence of the spectra on heterostructure parameters such as DMS-layer thickness and the materials adjacent to the DMS layer. The 3 T spectrum of an $In_{0.88}Mn_{0.12}As$(19 nm)/AlSb(145 nm) sample [Fig. 8(a)] shows only a weak feature α at 1.8 eV. The maximum θ_K has shifted down to 1.25 eV (peak β) as compared to the sample with a thinner DMS layer [Fig. 6(a)]. However, an S-shaped structure γ is observed again at 2.55 eV. Furthermore, two small features (δ,λ) can be distinguished at 0.85 and 2.2 eV, respectively. The remanence spectrum is only about 50% of the spectra at 3 T but all features are preserved.

In Fig. 8(b), the saturation and remanence spectra of an $In_{0.88}Mn_{0.12}As$(9 nm)/GaSb(600 nm) heterostructure are depicted. As in the case of the $In_{0.88}Mn_{0.12}As$(9 nm)/AlSb(136 nm) sample (Fig. 6), the remanence spectrum is almost identical to the one at 3 T, yielding a squareness of the Kerr hysteresis loops close to 1. However, the spectral dependence is quite different from Fig. 6. There is no sharp structure with the exception of an S-shaped feature (peak γ) at 2.6

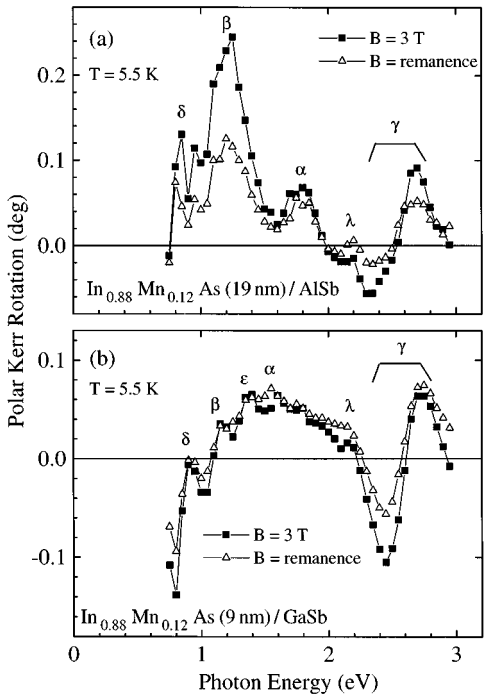

FIG. 8. Polar Kerr-rotation spectra at 5.5 K of (a) an $In_{0.88}Mn_{0.12}As(19\ nm)/AlSb(145\ nm)$ heterostructure and (b) an $In_{0.88}Mn_{0.12}As(9\ nm)/GaSb(600\ nm)$ heterostructure as a function of photon energy in a field of 3 T (■) and in the remanence state (△).

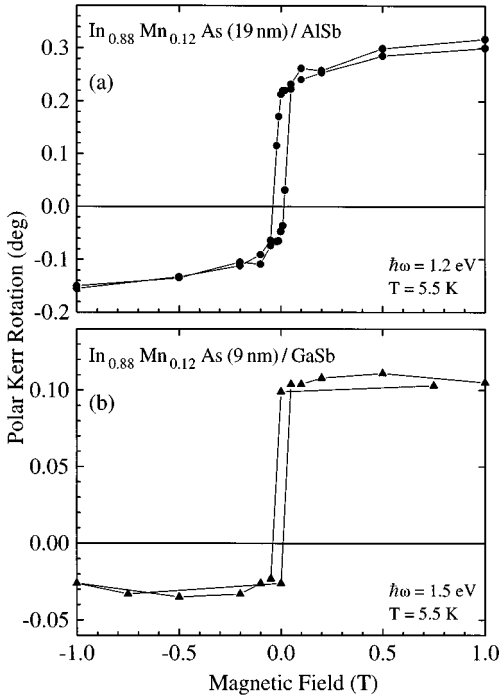

FIG. 9. Polar Kerr hysteresis loops at 5.5 K of (a) an $In_{0.88}Mn_{0.12}As(19\ nm)/AlSb(145\ nm)$ heterostructure and (b) an $In_{0.88}Mn_{0.12}As(9\ nm)/GaSb(600\ nm)$ heterostructure at a photon energy $\hbar\omega$=1.2 and 1.5 eV, respectively.

eV. The rest of the Kerr spectra is dominated by a broad peak α at 1.5 eV with a few small features ($\beta,\delta,\varepsilon,\lambda$) on top of it.

Polar Kerr hysteresis loops of (a) the (In,Mn)As/AlSb sample with 19 nm DMS-layer thickness and of (b) the (In,Mn)As/GaSb sample are shown in Fig. 9 at a photon energy of, respectively, 1.2 and 1.5 eV which corresponds to the maximum θ_K in these samples. A reduced squareness is clearly seen in Fig. 9(a). The coercive field amounts in both heterostructures to $H_c \cong 0.03$ T which is only half the value of H_c in the (In, Mn)As/AlSb sample with 9 nm thick DMS layer (Fig. 7). Such a reduction in coercivity has been observed before in Hall measurements.[8]

The influence of an $In_{0.5}Al_{0.5}As$-spacer layer on the Kerr rotation is shown in Fig. 10 for a spacer-layer thickness d_{sp}=3.5, 7, and 24 nm. The spectra are measured in (a) a magnetic field of 3 T capable of saturating the samples and (b) in the remanent state. At 3 T [Fig. 10(a)], θ_K reaches its maximum at 1.45 eV in the heterostructures with d_{sp}=3.5 and 7 nm (peak α). The sample with the thickest spacer layer d_{sp}=24 nm does not show a peak at that photon energy but reaches a maximum θ_K at 1 eV (peak β). An S-shaped structure (peak γ) centered at 2.55 eV is found in all three samples with spacer layer. Looking at the remanence spectra [Fig. 10(b)], a Kerr rotation of 25% of the saturation value is obtained for the sample with the thinnest spacer layer (d_{sp}=3.5 nm), whereas for the sample with d_{sp}=7 and 24 nm only 14% is reached. Because of the small θ_K values, a remanence rotation can only be separated from noise in the latter samples at 1.45 and 1 eV, respectively, where θ_K reaches its maximum value.

The change in the polar Kerr hysteresis loops with spacer-layer thickness d_{sp} is demonstrated in Fig. 11. The loops are taken at the photon energy of the maximum θ_K. The squareness as well as the coercivity decreases with increasing d_{sp}. While H_c=0.02 T for d_{sp}=3.5 nm, it decreases to H_c=0.015

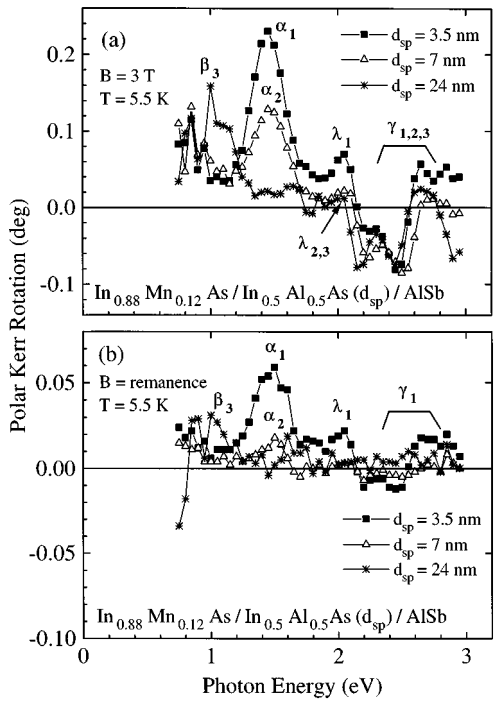

FIG. 10. Polar Kerr-rotation spectra as a function of photon energy at 5.5 K of $In_{0.88}Mn_{0.12}As/In_{0.5}Al_{0.5}As(d_{sp})/AlSb$ heterostructures with $In_{0.5}Al_{0.5}As$-spacer layer thickness d_{sp}=3.5 nm (■), 7 nm (△), and 24 nm (∗). The spectra are measured in (a) a field of 3 T and (b) in the remanence state.

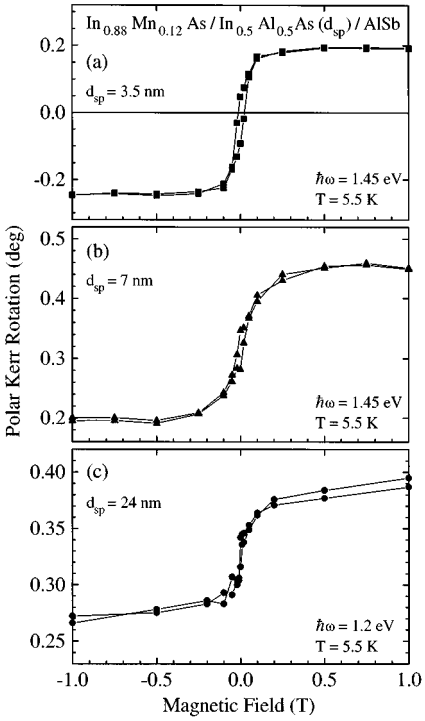

FIG. 11. Polar Kerr hysteresis loops at 5.5 K of $In_{0.88}Mn_{0.12}As/In_{0.5}Al_{0.5}As(d_{sp})/AlSb$ heterostructures with an $In_{0.5}Al_{0.5}As$-spacer layer thickness $d_{sp}=3.5$ nm (a), 7 nm (b), and 24 nm (c) at a photon energy $\hbar\omega=1.45$, 1.45, and 1.2 eV, respectively.

T for $d_{sp}=7$ nm and vanishes for $d_{sp}=24$ nm. However, even for the heterostructure with the thickest spacer layer investigated in this work a typical ferromagnetic hysteresis curve is found which is in apparent contradiction to Hall measurements on these samples.[6]

DISCUSSION

Correlation between reflectivity and Kerr spectra

The very structured reflectivity spectra of the heterostructures have a considerable influence on the spectral dependence of the Kerr rotation. In order to separate the effects due to the reflectivity—or, more precisely, due to the optical functions n and k—from intrinsic magneto-optically active electronic transitions, one has to define a quantity which represents the intrinsic magneto-optic activity. Such a quantity is the off-diagonal element $\tilde{\sigma}_{xy}$ of the complex optical conductivity tensor

$$\tilde{\sigma}=\begin{pmatrix} \tilde{\sigma}_{xx} & \tilde{\sigma}_{xy} \\ -\tilde{\sigma}_{xy} & \tilde{\sigma}_{xx} \end{pmatrix}, \tag{2}$$

where $\tilde{\sigma}_{ij}=\sigma_{1ij}+i\sigma_{2ij}$. In Eq. (2) the magnetization of the sample and the direction of the light beam are along the z axis and the sample surface is in the xy plane. The off-diagonal elements $\tilde{\sigma}_{xy}$ are to first order proportional to the joint density of states, $J_{\alpha\beta}$ of initial (α) and final (β) electronic state.[15] As a consequence, $\tilde{\sigma}_{xy}$ is proportional to the product of density of states of initial (n_α) and final (n_β) state times the joint spin density s_j:

$$s_j=\frac{s_{\alpha\uparrow}s_{\beta\uparrow}-s_{\alpha\downarrow}s_{\beta\downarrow}}{s_{\alpha\uparrow}s_{\beta\uparrow}+s_{\alpha\downarrow}s_{\beta\downarrow}}. \tag{3}$$

This leads in general to the well-known proportionality between polar Kerr rotation and perpendicular component of the magnetization of the sample. The relation between $\tilde{\sigma}_{xy}$ and the experimentally accessible Kerr effect, $\tilde{\theta}_K=\theta_K-i\eta_K$, where θ_K and η_K are the Kerr rotation and ellipticity, respectively, is given by the following formula:[11]

$$\tilde{\theta}_K=\frac{4\pi i}{\omega}\frac{\tilde{\sigma}_{xy}}{\tilde{n}(1-\tilde{n}^2)}, \tag{4}$$

where $\tilde{n}=n-ik$ is the complex *relative* index of refraction and ω is the frequency of the light. Note that relative index of refraction means the ratio of the indexes of refraction of the two media which form the interface where the light is reflected off. Thus $\tilde{n}$ is identical with the complex index of refraction of the magneto-optic material itself only for a surface facing vacuum.

As is evident from Eq. (4), the Kerr effect is not simply proportional to $\tilde{\sigma}_{xy}$, but depends in a nonlinear way on $\tilde{n}$. In the case of $\tilde{n}\cong 1$, an enhancement in $\tilde{\theta}_K$ will occur, which is called an optical-enhancement effect. Such a condition is given, e.g., near the plasma edge of a metal where the reflectivity reaches a minimum. A plasma-edge enhancement has been observed in the rare-earth chalcogenides TmS, TmSe, and NdS.[16,17] Because $\tilde{n}$ is the *relative* complex index of refraction in Eq. (4), an optical-enhancement effect can also be produced by an appropriate layer adjacent to the magneto-optic material. We strongly believe that this is the situation in the heterostructures described in this work.

By comparing the position of the major peak α in the Kerr spectra of the $In_{0.88}Mn_{0.12}As$(9 nm)/AlSb (Fig. 6) and of the $In_{0.88}Mn_{0.12}As$(9 nm)/$In_{0.5}Al_{0.5}As(d_{sp})$/AlSb samples (Fig. 10) with the position of the features in the corresponding reflectivity spectra (Figs. 4 and 5), we see that peak α lies at a photon energy where the reflectivity R goes through a local minimum before reaching its maximum at peak A. A similar correspondence is found in the heterostructures with a 19 nm thick DMS layer. Here, the main feature β of the Kerr spectra [Figs. 8(a) and 10] corresponds again to a local minimum in R (Figs. 4 and 5) before R reaches a local maximum at peak E. The exception is the (In,Mn)As(9 nm)/GaSb sample which shows only a broad feature A in the reflectivity (Fig. 3) and, accordingly, a broad peak α in the Kerr rotation [Fig. 8(b)]. This is probably due to the light absorption in the GaSb layer whose band gap is 0.81 eV.

In order to understand this agreement between peak position in the Kerr spectra and local minimum in reflectivity, we have to separate Eq. (4) into real and imaginary part:

$$\theta_K=F_2\sigma_{1xy}+F_1\sigma_{2xy}, \tag{5}$$

$$\eta_K=F_1\sigma_{1xy}-F_2\sigma_{2xy}, \tag{6}$$

where F_1 and F_2 are the magneto-optic scaling factors:

$$F_1=\frac{4\pi}{\omega}\frac{A}{A^2+B^2}, \tag{7}$$

TABLE II. Parameters of the Lorentzian curves, $\tilde{\varepsilon}_{\mathrm{Lor}}=1+\omega_{pi}^2/[(\omega_{0i}^2-\omega^2)+i\omega\gamma_i]$, used to calculate the reflectivity spectrum of Fig. 12. Curves 2 and 3 represent the major transitions while curves 1 and 4 serve to approximate the influence of the remaining part of the reflectivity spectrum.

No.	ω_{0i} (eV)	ω_{pi} (eV)	γ_i (eV)
1	1.0	3	3
2	1.5	2	0.25
3	2.15	3	0.25
4	3.3	8	2

$$F_2=\frac{4\pi}{\omega}\frac{B}{A^2+B^2}, \tag{8}$$

and A and B are polynomial functions of n and k:

$$A=n^3-3nk^2-n, \tag{9}$$

$$B=-k^3+3n^2k-k. \tag{10}$$

To demonstrate the influence of the magneto-optic scaling factors F_1 and F_2 on the Kerr rotation θ_K, we approximate a reflectivity spectra which is typical for the heterostructures by four Lorentzian curves using the parameters given in Table II. The calculated reflectivity spectra R is plotted in Fig. 12 as a solid line. Let us assume that the off-diagonal elements σ_{1xy} and σ_{2xy} are slowly varying functions with photon energy and—for simplicity—that they are equal in magnitude. Then the spectral dependence of θ_K is given by the difference or sum of F_1 and F_2 depending on the relative sign of σ_{1xy} and σ_{2xy}. The result is shown in Fig. 12 as a dashed line (F_1+F_2) and a dotted line (F_2-F_1). Obviously, both combinations of the magneto-optical scaling factors show a sharp peak close to the minimum of R which proves the general correlation between local minimum in the reflectivity spectrum and peak position in θ_K. If σ_{1xy} and σ_{2xy} are themselves varying with photon energy, the two effects combine to yield a more complicated structure in θ_K.

The situation is different in the case of the S-shaped feature γ which appears in all Kerr spectra. It relates to the structures D and D' in the reflectivity spectra. But although D and D' are just minor features in R with a peak-to-valley difference of less than 5%, the S-shaped feature γ is equal in magnitude to the major peaks α and β in θ_K or even dominates the Kerr spectrum as in the case of $In_{0.88}Mn_{0.12}As/GaSb$ [Fig. 8(b)]. This indicates that the S-shaped feature is due to an intrinsic magneto-optic structure in $\tilde{\sigma}_{xy}$ and not to an optical-enhancement effect. This finding is corroborated by the appearance of an S-shaped feature in an inhomogeneous bulk (In,Mn)As sample.[9] Magneto-optically active electronic transitions involving the Mn $3d$ band are also found in the same photon-energy range in ferromagnetic perovskite-type $La_{1-x}(Ba,Sr)_xMnO_3$ thin films.[18]

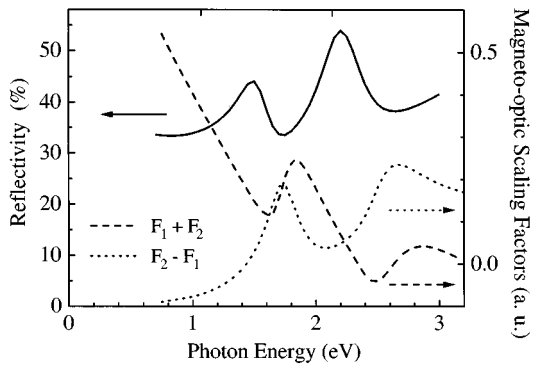

FIG. 12. Calculated reflectivity spectrum (solid line) using four Lorentzian functions as described in the text. The dashed and dotted lines are, respectively, the sum and difference of the two magneto-optic scaling factors F_1 and F_2 which are defined in Eqs. (7) and (8).

Thickness and interlayer dependence of ferromagnetic order

Although the energy dependence of the Kerr spectra is influenced by the optical functions n and k, the magnetic-field dependence of θ_K is solely due to spin-polarized electronic states which are contributing to the magnetic moment and give rise to an off-diagonal conductivity, $\tilde{\sigma}_{xy}$. A large remanent value of θ_K is observed, which amounts in some samples [Figs. 6 and 8(b)] to 100% of the saturation value over the entire photon energy range. This indicates that electronic transitions involving ferromagnetically ordered spins are magneto-optically active over the complete photon-energy range measured in this work.

There are two different types of electronic transitions which contribute to $\tilde{\sigma}_{xy}$: *inter*band and *intra*band transitions which display a different photon-energy dependence. The contribution to $\tilde{\sigma}_{xy}$ of intraband transitions, i.e., transitions within the conduction band for n-type and the valence band for p-type charge carriers, can be calculated using a phenomenological magneto-optic theory:[15,16]

$$\tilde{\sigma}_{xy}^{\mathrm{intra}}(\omega)=\frac{\omega_p^2 s_{\mathrm{cond}}}{4\pi}\left[-\frac{\Omega}{\Omega^2+(\gamma+i\omega)^2}+\frac{P_0}{ev_0}\left(1-\frac{i\omega(\gamma+i\omega)}{\Omega^2+(\gamma+i\omega)^2}\right)\right], \tag{11}$$

where ω_p is the plasma frequency, s_{cond} is the spin polarization, and v_0 is the Fermi velocity of the charge carriers. P_0 is a macroscopic dipole moment caused by the spin-orbit interaction, and γ and Ω are the relaxation and skew-scattering frequency, respectively.[15] By separating Eq. (11) into real and imaginary parts, the high-frequency limits of σ_{1xy} and σ_{2xy} can be derived:

$$\sigma_{1xy}(\omega\to\infty)\propto c_1\omega^{-2},\quad \sigma_{2xy}(\omega\to\infty)\propto c_2\omega^{-1}+c_3\omega^{-3}, \tag{12}$$

with the constants c_i depending on the parameters defined in Eq. (11). Consequently, intraband contribution to the Kerr spectra will be negligible at higher photon energies. By evaluating the parameters involved in Eqs. (11) and (12), a typical threshold photon energy of 1 eV can be estimated.[15,16] Hence, the Kerr spectra of the (In,Mn)As heterostructures are dominated by *inter*band transitions because spin-polarized electronic transitions are magneto-optically active over the whole photon-energy range.

The magnetization is due to localized, spin-polarized Mn $3d$ electrons. The magnetic exchange is mediated by holes which are spread in both the (In,Mn)As and AlSb layers, and of quasi-two-dimensional nature.[8] The hole states participating in the magnetic exchange will become spin-polarized themselves. Therefore, magneto-optically active interband transitions will involve in one way or another these electronic states.

The Mn ions are surrounded by six As ions similar to the NiAs structure of bulk MnAs.[19,20] Magneto-optically active transitions are hence transitions between the Mn $3d$ and the As $4p$ band and vice versa. Such transitions are expected to be very strong because they are dipole-allowed, highly spin-polarized and their radial overlap integral is large due to a high coordination number and small Mn-As distance. Furthermore, the transitions are rather broad because the width of the p and d band is usually more than 1 eV.

In conclusion, the Kerr-rotation spectra are due to electronic interband transitions confined to the (In,Mn)As layer. Magneto-optic spectroscopy therefore probes the magnetic behavior of exclusively the Mn $3d$ local moments.

With the help of the observed results, we are able to discuss the influence of DMS-layer and interlayer thickness on the ferromagnetic exchange. By comparing the magneto-optic hysteresis curves of (In,Mn)As/AlSb heterostructures with DMS-layer thickness $d_{\mathrm{MS}}=9$ nm (Fig. 7) and 19 nm [Fig. 9(a)], we find that the coercive field H_c decreases by a factor of 2 with increasing d_{MS}. Furthermore, the squareness, $\theta_K^{\mathrm{rem}}/\theta_K^{\mathrm{sat}}$ decreases from 100 to 60 %. A heterostructure with a 9 nm thick DMS layer grown on a GaSb layer [Fig. 9(b)], however, displays a squareness of 100%, while H_c is reduced to half the value of the corresponding (In,Mn)As/AlSb heterostructure (Fig. 7). This indicates a strong correlation between perpendicular magnetic anisotropy and strain-induced crystal anisotropy caused by a lattice mismatch of 0.6 and 1.3 % between the DMS layer and, respectively, the GaSb and AlSb layer.[8]

Finally, we now discuss the influence on the ferromagnetic exchange of an $In_{0.5}Al_{0.5}As$-spacer layer between the (In,Mn)As and AlSb layers. Introducing an $In_{0.5}Al_{0.5}As$ spacer layer leads to a pronounced decrease in coercivity and hysteresis behavior in the Hall resistance[6] indicating a disappearance of ferromagnetic order with increasing spacer-layer thickness d_{sp}. This observation has prompted the idea of carrier-induced ferromagnetism across the (In,Mn)As/AlSb interface[6] involving two-dimensional hole states specifically in the AlSb layer. The basic idea is that the holes in the AlSb layer would establish a Ruderman-Kittel-Kasuya-Yoshida-like exchange interaction with the Mn ions in the (In,Mn)As layer which would lead to long-range ferromagnetic order. A spacer layer acting as a potential barrier will suppress the penetration of the hole wave function into the (In,Mn)As layer and therefore reduce the ferromagnetic exchange between the Mn ions. Nevertheless, the corresponding Kerr hysteresis loops, which are plotted in Fig. 11, clearly demonstrate ferromagnetic order even in a heterostructure with $d_{\mathrm{sp}}=24$ nm, where the Hall resistivity gives just a linear dependence on magnetic field. Because the Kerr rotation is only sensitive to the (In,Mn)As layer, as has been justified above, it is concluded that the $In_{0.5}Al_{0.5}As$ interlayer does not upset ferromagnetic ordering but suppresses perpendicular magnetic anisotropy. The disappearance of low-field hysteretic behavior in the Hall resistance for the $d_{\mathrm{MS}}=24$ nm sample[6] may be explained in terms of parallel conduction due to two hole channels in both (In,Mn)As and AlSb layers, which sometimes occurs in modulation-doped (Ga,Al)As/GaAs heterostructures with heavy doping. In summary, we can conclude that the ferromagnetic exchange between the Mn $3d$ local moments is carried by the hole states within the (In,Mn)As layer.

CONCLUSIONS

III-V (In,Mn)As-DMS heterostructures show interesting optical, magneto-optic, and magnetic properties which warrant further investigation. The reflectivity spectra show a rich structure which originates from the layered arrangement of the samples. The spectral dependence of the Kerr rotation θ_K is strongly influenced by the reflectivity. From an analysis of the field dependence it is concluded that the Kerr rotation probes only the magnetic behavior within the (In,Mn)As layer.

The dependence of θ_K on DMS-layer thickness and the (Ga,Al)Sb underlayer yields a correlation between lattice mismatch and perpendicular magnetic anisotropy. From the variation of the Kerr hysteresis loops as a function of (In,Al)As-interlayer thickness it is deduced that the ferromagnetic exchange between the local Mn $3d$ magnetic moments is carried by hole states within the (In,Mn)As layer and not, as proposed before,[6] by an exchange across the (In,Mn)As/AlSb heterointerface involving two-dimensional hole states in the AlSb layer.

ACKNOWLEDGMENTS

This work has been partially supported by the TEPCO Research Foundation, the TORAY Science Foundation, the Grant-in-Aid for General Scientific Research No. 07455006, the Grant-in-Aid for Developmental Scientific Research No. 07555004, and the NEDO Research Project for the Development of New Materials.

[1] H. Munekata, H. Ohno, S. von Molnár, A. Segmüller, L. L. Chang, and L. Esaki, Phys. Rev. Lett. **63**, 1849 (1989).

[2] H. Munekata, H. Ohno, S. von Molnár, A. Harwit, A. Segmüller, and L. L. Chang, J. Vac. Sci. Technol. B **8**, 176 (1990).

[3] S. von Molnár, H. Munekata, H. Ohno, and L. L. Chang, J. Magn. Magn. Mater. **93**, 356 (1991).

[4] H. Munekata, H. Ohno, R. R. Ruf, R. J. Gambino, and L. L. Chang, J. Cryst. Growth **111**, 1011 (1991).

[5] H. Ohno, H. Munekata, T. Penney, S. von Molnár, and L. L. Chang, Phys. Rev. Lett. **68**, 2664 (1992).

[6] H. Munekata, T. Penney, and L. L. Chang, Surf. Sci. **267**, 342 (1992).

[7] H. Ohno, H. Munekata, S. von Molnár, and L. L. Chang, J. Appl. Phys. **69**, 6103 (1991).

[8] H. Munekata, A. Zaslavsky, P. Fumagalli, and R. J. Gambino, Appl. Phys. Lett. **63**, 2929 (1993).

[9] P. Fumagalli, H. Munekata, and R. J. Gambino, IEEE Trans. Magn. **29**, 3411 (1993).
[10] S. Guha and H. Munekata, J. Appl. Phys. **74**, 2974 (1993).
[11] W. Reim and J. Schoenes, in *Handbook of Ferromagnetic Materials*, edited by K. H. J. Buschow and E. P. Wohlfarth (North-Holland, Amsterdam, 1990), Vol. 5, p. 133.
[12] D. Y. Smith, E. Shiles, and M. Inokuti, in *Handbook of Optical Constants of Solids*, edited by E. A. Palik (Academic, New York, 1991), Vol. I, pp. 369.
[13] O. Madelung, W. von der Osten, and U. Rössler, in *Intrinsic Properties of Group IV Elements and III-V, II-VI and I-VII Compounds*, edited by O. Madelung, Landolt-Börnstein, New Series, Vol. NS III/22a (Springer, Berlin, 1987).
[14] S. Adachi, J. Appl. Phys. **66**, 6030 (1989).
[15] J. L. Erskine and E. A. Stern, Phys. Rev. B **8**, 1239 (1973).
[16] W. Reim, O. E. Hüsser, J. Schoenes, E. Kaldis, and P. Wachter, J. Appl. Phys. **55**, 2155 (1984).
[17] H. Brändle, J. Schoenes, and F. Hulliger, Helv. Phys. Acta **62**, 199 (1989).
[18] P. Fumagalli, C. Spaeth, G. Güntherodt, R. von Helmolt, and J. Wecker, IEEE Trans. Magn. **31**, 3277 (1995).
[19] A. Krol, Y. L. Soo, S. Huang, Z. H. Ming, Y. H. Kao, H. Munekata, and L. L. Chang, Phys. Rev. B **47**, 7187 (1993).
[20] H. Munekata, L. L. Chang, A. Krol, Y. L. Soo, S. Huang, Z. H. Ming, and Y. H. Kao, J. Cryst. Growth **127**, 528 (1993).